Selected Applications of the Macroscopic-Microscopic Method

Kasia MAZUREK

Institute of Nuclear Physics
Polish Academy of Sciences, Kraków, Poland

March 2, 2012

Outline

- Macroscopic-Microscopic Method

a) Shell and Pairing Energies
b) Macroscopic Models

- Applications

a) Shape Coexistence
b) Islands of Inversion
c) Rotational Bands
d) Superdeformation
e) Giant Dipole Resonance
f) Fission Dynamics

- Summary

Macroscopic-Microscopic Method

$$M(Z,N;def) = ZM_H + NM_n - 0.00001433Z^{2.39}$$
$$+E_{LSD}(Z,N;def) + E_{micr}(Z,N;def)$$

Macroscopic Energy: Lublin - Strasbourg Drop, Finite Range Liquid Drop Model Microscopic Energy

$$E_{micr} = E_{pair} + E_{shell}$$

'Pairing' Energy

$$E_{pair} = E_{BCS} + \overline{E}_{pc}$$

Woods-Saxon Single-Particle Potential

[S. Ćwiok, J. Dudek, W. Nazarewicz, J. Skalski, T. Werner, Comp. Phys Comm **46** (1987) 379]

$$\langle \nu | h(1) | \mu \rangle = e_\nu \delta_{\nu\mu}$$

$$h(1) \Rightarrow \hat{H}_{WS} = \hat{t} + \hat{V}_{WS} \Rightarrow \hat{V}_{WS} = \hat{V}_{cent} + \hat{V}_{so} + \hat{V}_{Coul}$$

$$\hat{V}_{cent}(\vec{r}; V_0, \kappa, a, r_0) = \frac{V_0 \left[1 \pm \kappa \frac{N-Z}{N+Z}\right]}{\left\{1 + \exp\left[\mathrm{dist}_{\Sigma_0(\vec{r}, r_0)}/a\right]\right\}}; \quad V_{Coul} = \begin{cases} \frac{Ze^2}{r} \\ \frac{Ze^2}{2R_0}\left[3 - \left(\frac{r}{R_0}\right)^2\right] \end{cases}$$

The spin-orbit term:

$$\hat{V}_{so}(\vec{r}, \vec{p}; V_0^{so}, \kappa, a_{so}, r_{so}) = \lambda \left[\frac{\hbar}{2mc}\right]^2 \left[\vec{\nabla} \frac{V_0^{so}\left[1 \pm \kappa \frac{N-Z}{N+Z}\right]}{1 + \exp\left[\mathrm{dist}_{\Sigma_{so}(\vec{r}, r_{so})}/a_{so}\right]}\right] \times \vec{p} \cdot \vec{s};$$

$$V_0^{so} = \lambda \left[\frac{\hbar}{2mc}\right]^2 V_0 \left[1 \pm \kappa \frac{N-Z}{N+Z}\right]; \quad R_0 = r_0 A^{1/3}$$

Macroscopic-Microscopic Method

Single-particle levels

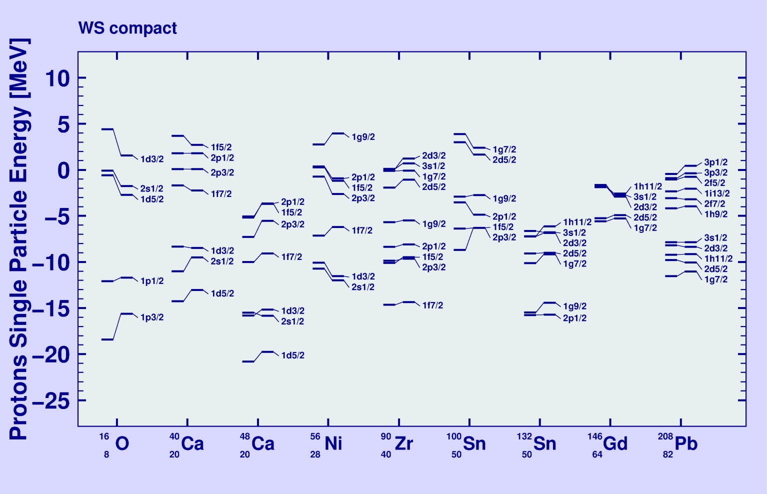

Comparison of the calculated (right) and experimental (left) single-particle levels

- new UNIVERSAL-DIRAC parameters. (PhD thesis of N. Dubray)

Strutinski Shell Energy

$$E_{shell} = \sum_{n=1}^{N} e_n - \int_0^N \bar{e}_n(n)dn$$

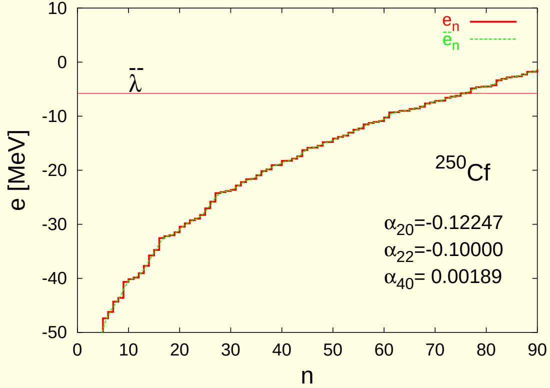

Pairing Energy

$$E_{pair} = E_{BCS} + \overline{E}_{pc}$$

$$E_{BCS} = \sum_{\nu=\mathcal{N}_1}^{\mathcal{N}_2} 2v_\nu^2(e_\nu - \lambda) - \frac{\Delta^2}{G} - G\left(\sum_{\nu=\mathcal{N}_1}^{\mathcal{N}_2} v_k^4 - \sum_{\nu=\mathcal{N}_1}^{\mathcal{N}_2} 1\right) - \sum_{\nu=\mathcal{N}_1}^{\mathcal{N}_2} (e_\nu - \lambda)$$

$$\overline{E}_{pc} = -\frac{1}{4}\frac{N^2}{\overline{\rho}}\left\{\left[1 + \left(\frac{2\overline{\rho}\overline{\Delta}}{N}\right)^2\right]^{1/2} - 1\right\} + \frac{1}{2}\overline{\rho}\overline{\Delta G}\arctan\frac{N}{2\overline{\rho}\overline{\Delta}}$$

$$\overline{\Delta}_n = 9.08/\sqrt{A}, \quad \overline{\Delta}_p = 9.85/\sqrt{A}$$

Macroscopic-Microscopic Method

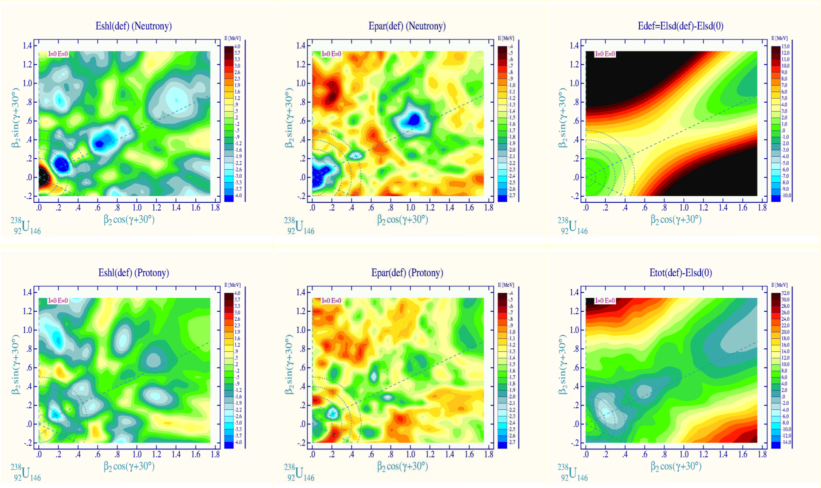

Macroscopic-Microscopic Method with Cranking

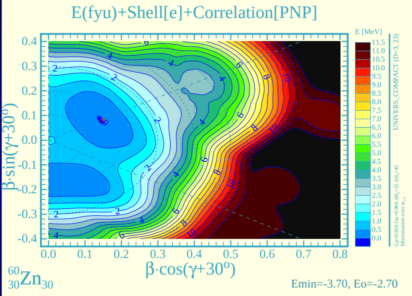

Total energy map

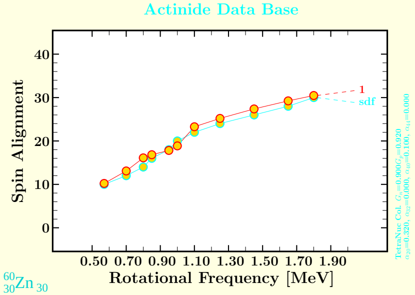

Spin alligment for the super deformed rotational band

$$\hat{H}^{\omega}_{WS} \quad = \quad \hat{H}_{WS} - \omega \cdot \hat{j}$$

Conclusions for the Macroscopic Models

- The nuclear surface energy comes from the nuclear matter contained in a certain surface region whose magnitude is determined by its diffusivity.

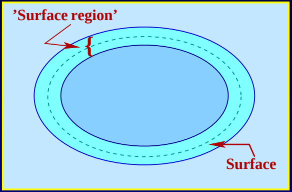

Figure: *For Steiner sheets and relatively thin skin (small surface region) the amount of nuclear matter contained in the surface region is approximately proportional to the volume of the surface region.*

- The volume of the 'surface region', $\mathcal{V}_S$, is approximated by

$$\mathcal{E}_{\mathrm{surf}} \sim \mathcal{V}_{\mathrm{S}} \sim \int_{s_1}^{s_2} \mathcal{S}(s)\,ds \sim \int_{s_1}^{s_2} [\mathcal{S}_0 + \mathcal{L}_0 s]\,ds$$

Conclusions for the Structure of $\mathcal{E}_{surf}$

- The nuclear surface energy can be decomposed into at least two terms whose **A**-dependences are different: $\mathbf{A^{2/3}}$ and $\mathbf{A^{1/3}}$

- At *the same surface area* $\mathcal{S}_0$ two nuclei differing by average curvatures $\mathcal{L}_0$ and $\mathcal{L}_0'$, *will have different surface energies*

- Since the proportionality coefficients $\mathcal{C}_S(Z, N)$ and $\mathcal{C}_L(Z, N)$ are in fact *'functions of the nucleus'*, it follows that in two different nuclear regions the relative proportions of the surface-area term to the surface-curvature term will be in general different (e.g. vanishing surface-curvature)

- The surface energy is proportional to the *volume of the surface region*

- There is no *a priori* statement about the sign of curvature contributions

The Physics of the Nuclear Surface

- The fit of parameters of the extended formula to 2772 masses improves the results for the barriers by better than a factor of 4 (!!)

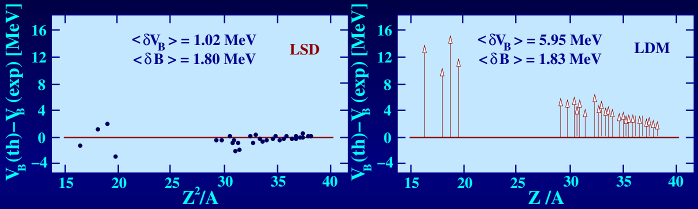

Figure: *Results of the fitting of the parameters to the experimental masses give simultaneously and improvement in the description of the experimental fission barriers (left); fit performed under the same conditions but without curvature terms ('traditional') is given for comparison on the right.*

K. Pomorski, J. Dudek, Phys. Rev. **C 67**,044316(2003)

Macroscopic energy calculations

- In the past, often the Yukawa-folded approach has been used;
- In such an approach the surface energy is obtained through a procedure using the Yukawa-folding function $F(|\vec{r} - \vec{r}'|, a)$

Macroscopic energy calculations

- In the past, often the Yukawa-folded approach has been used;
- In such an approach the surface energy is obtained through a procedure using the Yukawa-folding function $F(|\vec{r} - \vec{r}'|, a)$
- The diffuseness parameter a serves to collect the contributions from the nuclear surface region only

Macroscopic energy calculations

- In the past, often the Yukawa-folded approach has been used;
- In such an approach the surface energy is obtained through a procedure using the Yukawa-folding function $F(|\vec{r} - \vec{r}'|, a)$
- The diffuseness parameter a serves to collect the contributions from the nuclear surface region only
- The folding procedure results in a dangerous loss of sensitivity with respect to high-order multipoles

Macroscopic energy calculations

• In the past, often the Yukawa-folded approach has been used;

• In such an approach the surface energy is obtained through a procedure using the Yukawa-folding function $F(|\vec{r}-\vec{r}'|, a)$

• The diffuseness parameter a serves to collect the contributions from the nuclear surface region only

• The folding procedure results in a dangerous loss of sensitivity with respect to high-order multipoles

• Also the fission barrier-heights especially for the lighter nuclei do not correspond well with the experimental data

Macroscopic Energy Calculations: Stiffness Pathology

- The folding procedure and the optimally fitted parameters both result in a characteristic loss of sensitivity with respect to high-order multipoles: Stiffness remains weak at increasing multipolarity

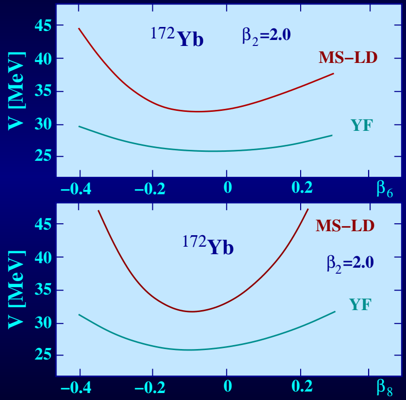

Figure: At large elongation, Yukawa-folded macroscopic energies depend relatively weakly on the higher order multipoles: β_6, β_8, β_{10}, etc.

The Final LSD Macroscopic Energy Expression

- *Mass-fits are improved slightly with respect to other models but the fission barriers are improved considerably;*
- *The fission barriers involve large deformations where the curvature of the nuclear surface plays an important role;*
- *This significant improvement confirms the right physics:*

$$\begin{aligned}
E_{lsd}(Z,N;def) &= b_{vol}\{1-\kappa_{vol}[(N-Z)/A]^2\}\,A \\
&+ b_{surf}\{1-\kappa_{surf}[(N-Z)/A]^2\}\,A^{2/3}B_{surf}(def) \\
&+ b_{curv}\{1-\kappa_{curv}[(N-Z)/A]^2\}\,A^{1/3}B_{curv}(def) \\
&+ \frac{3}{5}e^2\frac{Z^2}{r_0^{ch}A^{1/3}}B_{Coul}(def) \\
&+ E_{micr}(Z,N;def) \\
&+ E_{cong}(Z,N;def)
\end{aligned}$$

K. Pomorski, J. Dudek, Phys. Rev. **C 67**,*044316(2003),*

J. Dudek, K. Pomorski, N.Schunck, N. Dubray, Eur. Phys. J. **A 20**, *15 (2004)*

LSD - Some Illustrations

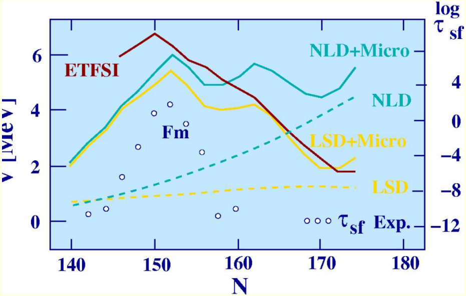

Comparison of the model results: Extended Thomas Fermi with Skyrme Interaction (ETFSI), Lublin-Strasbourg Drop (LSD) and the 'traditional' one (NLD). The logarithms of the spontaneus fission half lives are given for qualitative comparison (right scale)

• At high temperatures, the total nuclear energy can be approximated by the macroscopic energy expression only

• The angular momentum effects can be treated, to the first approximation classically

$$\mathrm{E}_{\mathrm{total}}(\{\mathrm{def.}\};\mathrm{I}) = \mathrm{E}_{\mathrm{macro}}(\{\mathrm{def.}\}) + \frac{\hbar^2}{2\mathcal{J}\{\mathrm{def.}\}} \cdot \mathrm{I}(\mathrm{I}+1)$$

• Conclusion:

Using the macroscopic energy as optimal as possible will be of importance: in our case $\longrightarrow$ the LSD Model

Macroscopic-Microscopic Method

Nuclear surface parametrization:

$$\mathcal{R}(\vartheta,\varphi) = R_0\, c(\{\alpha\}) \sum_{\lambda,\mu} [1 + \alpha_{\lambda,\pm\mu}\, Y_{\lambda,\pm\mu}(\vartheta,\varphi)]$$

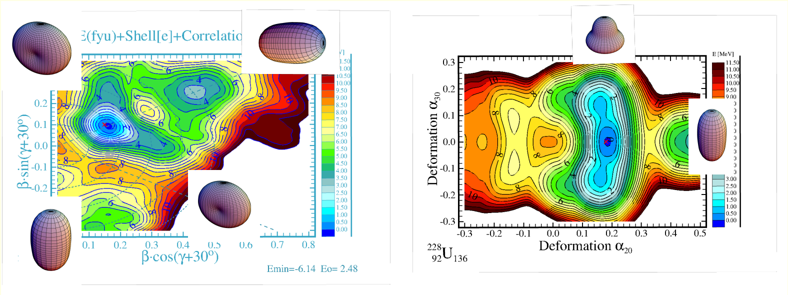

$\{\beta,\gamma\} \rightarrow \{\alpha_{20},\alpha_{22}\}$

Inversion Islands

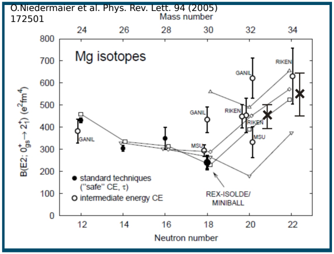

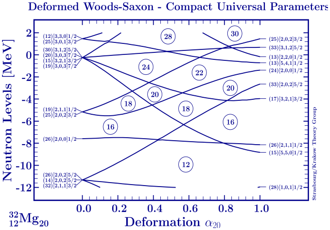

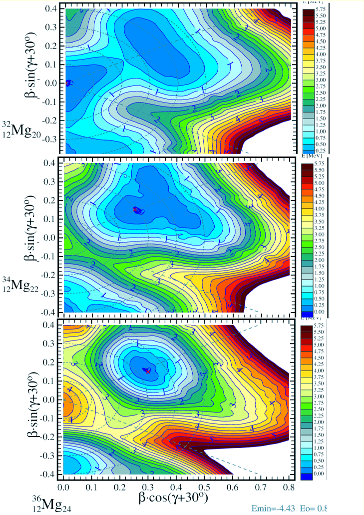

Applications → T=0, Low Spin

Shape coexistence

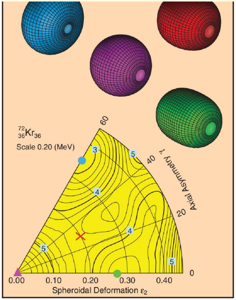

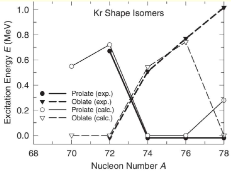

P. Moller PRL **103,** 212501 (2009)

M. Zielinska et al.
PHYSICAL REVIEW C **80**, 014317 (2009)

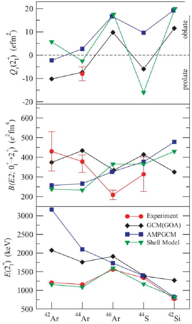

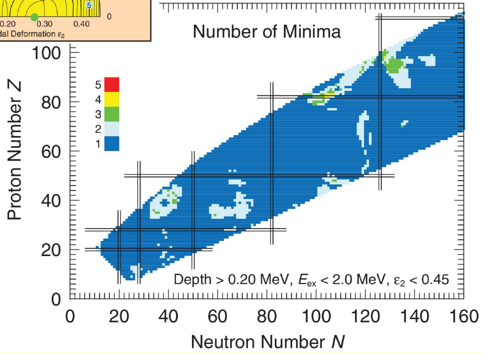

Applications → T=0, Low Spin

Rotational Bands- low spin *D. Curien et al. Phys. J. Phys. Conf. Ser. 205 (2010) 012034*

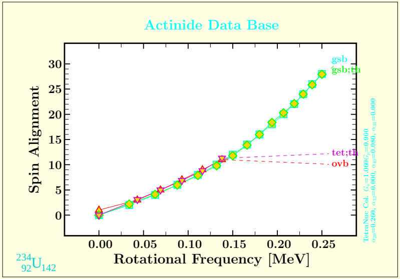

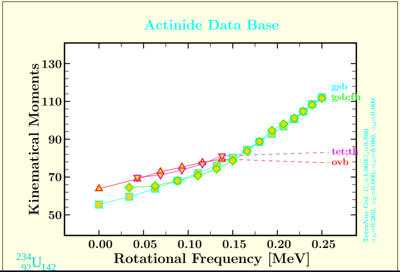

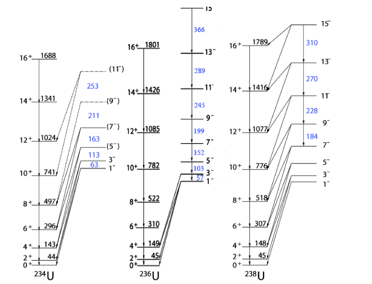

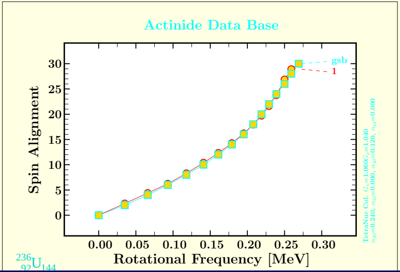

Superdeformation - ^{152}Dy

J.Dudek et al. Eur. Phys. J. A 20 (2004) 165; H. Savajols et al., Phys. Rev. Lett. 76, 4480 (1996)

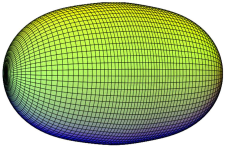

Fig. 1. The superdeformed nucleus ^{152}Dy, according to the measurements of ref. [8] has the quadrupole moment $Q_2 = 17.2$ eb. The corresponding deformation $\alpha_{20} = 0.61$ and $\alpha_{40} = 0.11$ obtained, *e.g.*, from the calculations with the Woods-Saxon potential as in ref. [9] reproduces the measured dynamical moments and the quadrupole moment. The shape presented in the figure corresponds to the above deformation.

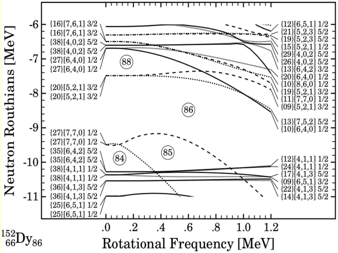

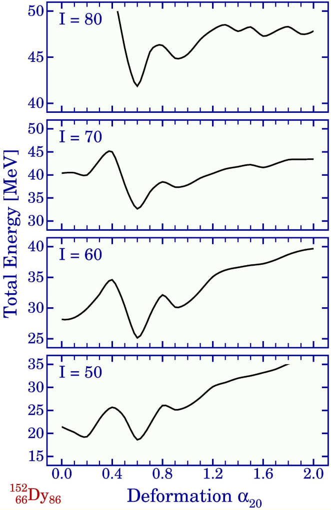

Giant Dipole Resonances-Jacobi Shape Transition.

Total energy minimum evolution with increasing the spin - ^{46}Ti.

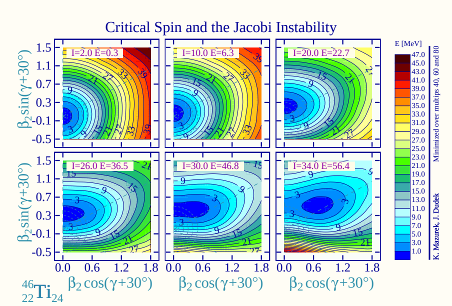

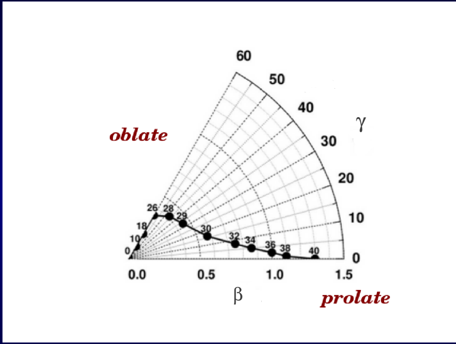

Spherical - oblate - nonaxial - prolate

A. Maj et al., Nucl. Phys. **A 731**, 319 (2004)

M. Kmiecik et al., Phys. Rev. **C 70**, 064317 (2004)

N. Schunck et al., Phys. Rev. **C 75**, 054304 (2007)

Giant Dipole Resonances

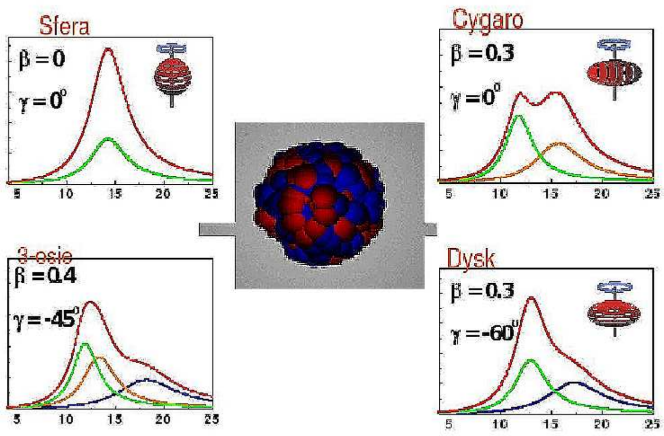

The shape evolution of the compound nucleus influents into the GDR strenght function. A. Maj et al., Nucl. Phys. **A 731**, 319 (2004)

Applications → T≠0, High Spin

Giant Dipole Resonances

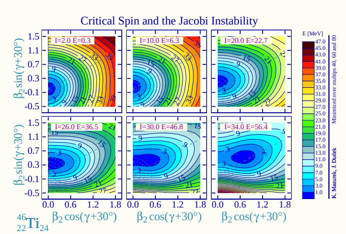

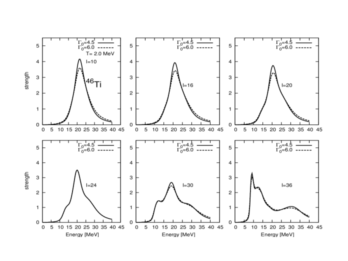

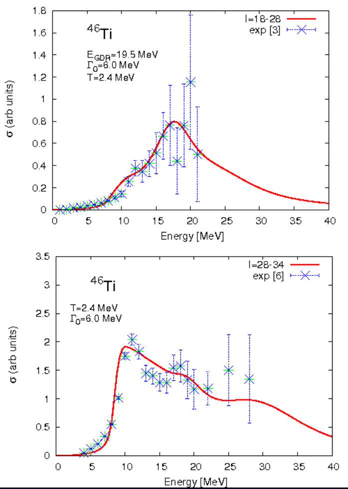

Eksperiment: A. Maj et al., Nucl. Phys. A 731, 319 (2004).

Applications → T=0, No Spin

Low-Energy Shape Oscillations

Low-energy shape oscillations

of negative parity

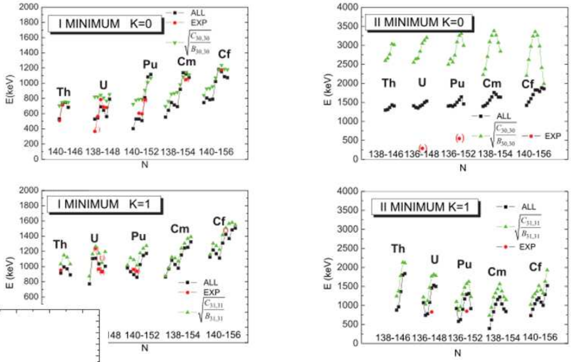

M. KOWAL AND J. SKALSKI
PHYSICAL REVIEW C **82**, 054303 (2010)

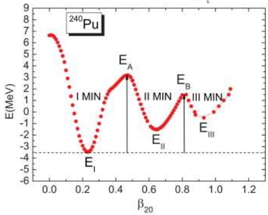

FIG. 1. (Color online) Calculated fission barrier for ^{240}Pu as a function of β_{20}.

Applications → T≠0, High Spin

Fission dynamics-Langevin equations

$$\frac{dq_i}{dt} = \sum_j [M^{-1}(\vec{q})]_{ij} p_j$$

$$\frac{dp_i}{dt} = -\frac{1}{2} \sum_{j,k} \frac{d[M^{-1}(\vec{q})]_{jk}}{dq_i} p_j p_k - \frac{dV(\vec{q})}{dq_i} - \sum_{j,k} \gamma_{ij}(\vec{q}) [M^{-1}(\vec{q})]_{jk} p_k + \sum_j g_{ij}(\vec{q}) \Gamma_j$$

- $[M^{-1}(\vec{q})]_{ij}$ - tensor ot inertia, M_{ij} - tensor of mass
- $V(\vec{q})$ - potential energy
- $\vec{q} = (q_1, q_2, g_3)$ - collective coordinates
- $\vec{p} = (p_1, p_2, p_3)$ - conjugate momenta
- $\Gamma_i(t)$ - random variable: $\langle \Gamma_i \rangle = 0$, $\langle \Gamma_i(t_1) \Gamma_j(t_2) \rangle = 2\delta_{ij}\delta(t_1 - t_2)$
- $D_{ij} = g_{ik} g_{kj} \equiv T\gamma_{ij}$ - diffusion tensor
- $T = [E_{int}/a(\vec{q})]^{1/2}$ - temperature from Fermi gas model
- E_{int} -internal excitation energy
- $E_{coll}(\vec{q}, \vec{(p)}) = \frac{1}{2}[M^{-1}(\vec{q})]_{ij} p_i p_j$ - the kinetic energy of the collective degrees of freedom
- $a(\vec{q}) = a_v A + a_s A^{2/3} B_s(\vec{q})$ - Ignatyuk level density parameter

Collective coordinates in " funny hills" parametrisation

$$q_1 = c$$
$$q_2 = \frac{h+3/2}{\frac{5}{2c^3}+\frac{1-c}{4}+3/2}$$
$$q_3 = \begin{cases} \alpha/(A_s+B), & B \geq 0 \\ \alpha/A_s, & B \leq 0 \end{cases}$$

$$\rho_s^2(z) = \begin{cases} (c^2-z^2)(A_s + Bz^2/c^2 + \frac{\alpha z}{c}), & B \geq 0 \\ (c^2-z^2)(A_s + \frac{\alpha z}{c}) exp(Bzc^2), & B \leq 0 \end{cases}$$

$$B = 2h + \frac{c-1}{2}$$
$$A_s = \begin{cases} c^{-3} - \frac{B}{5}, & B \geq 0; \\ -\frac{4}{3}\frac{B}{exp(Bc^3)+(1+\frac{1}{2Bc^3})\sqrt{-\pi Bc^3}\, erf(\sqrt{-Bc^3})}, & B \leq 0 \end{cases}$$

Applications

Potential Energy Surfaces (PES)

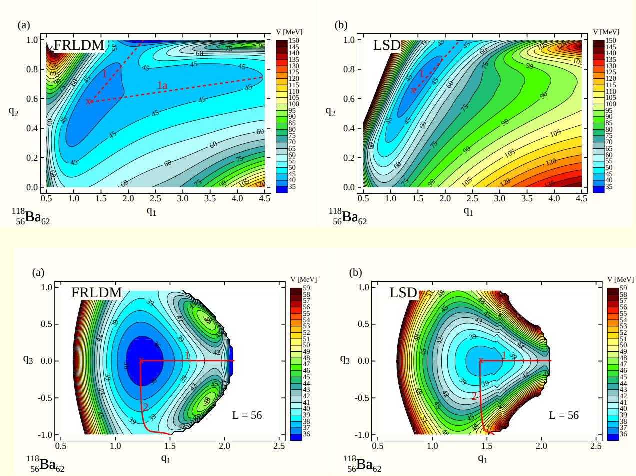

The potential energy surfaces for the ^{118}Ba calculated with the LSD (right) and the FRLDM model (left) in the plane (q_1, q_2)-top and (q_1, q_3)-bottom.

FF Charge distribution

G. Ademard et al., Phys. Rev. **C 83**, *054619 (2011)*

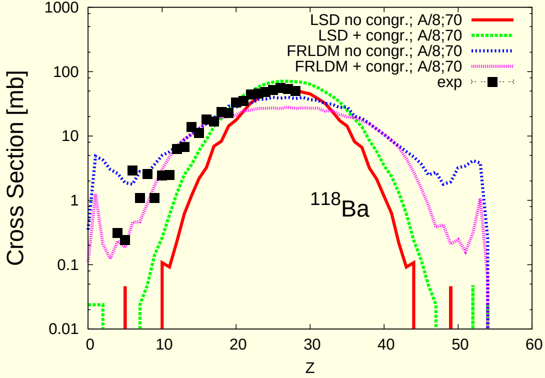

Z distribution for ^{118}Ba with angular momentum $l = 0-70\ \hbar$ for potential energy surfaces calculated with the LSD formula and FRLDM model and with constant density parameter a=A/8 with viscosity $k_s = 0.2$. The influence of the congruence (Wigner) energy is shown.

Applications

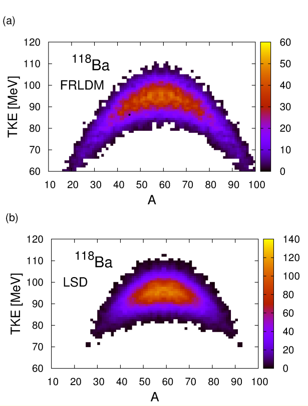

Correlation between the mass A and total kinetic energy TKE of the fission fragments produced in the reaction $^{78}Kr(429\ MeV)+^{40}Ca\to\ ^{118}Ba$. *The top (bottom) panel shows the calculation performed with the FRLDM (LSD) potential. In all calculations, the level-density parameter is* $a = A/8\ MeV^{-1}$ *and* k_s *is set to 0.2.*

	FRLDM	LSD
P_f	0.42	0.49
$\langle n_{pre}\rangle$	0.03	0.03
$\langle p_{pre}\rangle$	0.06	0.04
$\langle \alpha_{pre}\rangle$	0.03	0.03
$\langle n_{eva}\rangle$	1.31	1.38
$\langle p_{eva}\rangle$	3.00	3.09
$\langle \alpha_{eva}\rangle$	1.47	1.43
σ^2_A	371.86	126.13
σ^2_Z	83.82	28.69
$\langle TKE\rangle$	87.48	94.17
$\sigma^2_{E_k}$	197.13	35.83
$\langle T_{sc}\rangle$	1.67	1.68

K. M., C. Schmitt, J.P. Wieleczko, P.N. Nadtochy, G. Ademard, Phys. Rev. **C 84**, *014610 (2011)*

Summary and Conclusions

- *The MMM is very powerful method to estimate many experimental observables*
- *The nuclear shape deformation is easy investigated within this method*
- *The description of cold and excited nuclei can be done with reasonable precision*
- *The rotational bands and low-energy excitation can be also reproduced*